Latin American Journal of Solids and Structures
www.lajss.org

Damage based constitutive model for predicting the performance degradation of concrete

Abstract

An anisotropic elastic-damage coupled constitutive model for plain concrete is developed, which describes the concrete performance degradation. The damage variable, related to the surface density of micro-cracks and micro-voids, and represented by a second order tensor, is governed by the principal tension strain components. For adequately describing the partial crack opening/closure effect under tension and compression for concrete, a new suitable thermodynamic potential is proposed to express the state equations for modeling the mechanical behaviors. Within the framework of thermodynamic potential, concrete strain mechanisms are identified in the proposed anisotropic damage model while each state variable is physically explained and justified. The strain equivalence hypothesis is used for deriving the constitutive equations, which leads to the development of a decoupled algorithm for effective stress computation and damage evolution. Additionally, a detailed numerical algorithm is described and the simulations are shown for uni-axial compression, tension and multi-axial loadings. For verifying the numerical results, a series of experiments on concrete were carried out. Reasonably good agreement between experimental results and the predicted values was observed. The proposed constitutive model can be used to accurately model the concrete behaviors under uni-axial compression, tension and multi-axial loadings. Additionally, the presented work is expected to be very useful in the nonlinear finite element analysis of large-scale concrete structures.

Keywords

Anisotropic damage, concrete, constitution, nonlinear finite element analysis, thermodynamic potential, strain equivalence hypothesis

Zhi Wang[1]
Xianyu Jin[*1]
Nanguo Jin[1]
Abid A Shah[2]
Bei Li[1]
.
. xianyu@zju.edu.cn (Xianyu Jin)
[1]Department of Civil Engineering, Zhejiang University, Hangzhou 310027, China
[2]Department of Civil Engineering, University of Siegen, 57076 Siegen, German

1 INTRODUCTION

Concrete has been widely used in many civil engineering structures. Due to its ability of being cast easily into structural members of different shapes as arc, ellipsoid etc., the demand for concrete utilization in structures is increasing rapidly (Shah and Hirose, 2010; Shah et al., 2012). One of the most important characteristics of concrete is its higher strength in compression and lower in tension. This property leads to tensile cracking in concrete under very low stress that results into reducing the effective stiffness of concrete structural members. Additionally, concrete structures perform differently under uni-, bi-, and tri-axial loadings (Mazars, 1986). For example, compressive strength of concrete under bi-axial loading is greater than that for uni-axial loading. In addition, a concrete structure undergoes nonlinear deformations and accompanies certain perfor-

mance degradation phenomena before maximum stress under a design load is reached (Poinard et al., 2010; Richard et al., 2010). For this purpose, it is very important to understand the mechanical behavior of concrete under tension and compression, for uni-, bi-, and tri-axial loadings, respectively. The most commonly used theories for modeling the concrete damage mechanism include plasticity theory, fracture based approach and damage mechanics.

Plasticity theory, which has been mathematically established, is presently being widely used to model the metal's behavior for its internal slip process. Many researchers have just used plasticity theory to characterize the concrete behavior (Chen and Chen, 1975; Bazant, 1978; Dragon and Mroz. 1979; Schreyer, 1983; Chen and Buyukozturk, 1985; Onate et al, 1993; Voyiadjis and Abulebdeh, 1994; Karabinis and Kiousis, 1994; Menetrey and Willam, 1995; Grassl et al., 2002). Nielsen (2010) presented a review on plasticity application to model concrete behavior. Although the plasticity models are far superior to elastic approaches in representing hardening and softening characteristics, pure plasticity theory could not be applied to concrete due to its quasi-brittle characteristic. Because they fail to model the process of damage due to micro-cracks growth, such as the stiffness degradation, the unilateral effect, etc.

Fracture mechanics suggests another approach to describe localized damage as to be represented by the ideal discrete cracks with definite geometries and locations, and it has been extensively used in engineering practice (Krajcinovic, 1985). Unfortunately, before the appearance of macro-cracks in concrete there exist a lot of smeared micro-cracks whose geometries and locations could not be determined precisely. At the same time, the associated questions whether the J integrals and stress intensity factors are material parameters or not are far from being settled [18]. So, there are some difficulties to apply fracture mechanics for modeling concrete precisely.

For describing the macro-level response of a concrete structure, damage mechanics (depending if the damage is discrete or non-discrete) is usually classed into two methods: micro-mechanical damage (MD) method and continuum damage mechanics (CDM) approach. The MD models assume that the damage is discrete and stochastic. They have the advantage of being able to sustain heterogeneous structural details on micro-scale. Additionally, they allow a micro-mechanical formulation of the damage evolution equations based on the accurate micro-crack growth processes involved (Fanella and Krajcinovic, 1988; Bazant and Prat, 1988; Carol et al., 1991; Carol ett al., 1992). However, geometries and locations of the pre-define cracks should be assumed in advance.

Continuum damage mechanics (CDM) approach provides the constitutive and damage evolution equations within the framework of thermodynamics of irreversible processes, the internal state variable theory and relevant physical considerations (Mazars and Cabot, 1989). CDM also provides a powerful and general frame work for the derivation of consistent constitutive models suitable for many engineering materials, including concrete. When the CDM approach is used, the material heterogeneity (on the micro-scale) is supposed to be smeared out over the representative volume element (RVE). Then the concept of thermodynamic damage variable is applied in RVE. Generally, the physical interpretation of the damage variable is introduced as the specific damaged surface area (Kachanov, 1958). There are two cases of damage density of micro-cracks and micro-voids: scalar (isotropic) and tensor (anisotropic). Using scalar damage variable is the easiest treatment, which represents representing an isotropic state of concrete degradation (Mazars, 1984; Bazant and Cabot, 1988; Lemaitre and Lippmann, 1996). This approach allows the expression of efficient material models dealing with robust stress algorithms. It should be noted here that the notions of tensile damage and compressive damage are sometimes also introduced, respectively. These notations are inconsistent with the idea of the state of variables representing a micro-cracking pattern.

For accurately interpreting the concrete damage, anisotropic damage should be considered. It is attributed to the evolution of micro-cracks in concrete whereas damage in metals can be satisfactorily represented by a scalar damage variable (isotropic damage) for evolution of voids. General-

ly, the presence of orthogonal compressive stress, for concrete subjected to bi-axial stresses, will lead to a stiffer response and greater strength, while the presence of orthogonal tensile stress for concrete under tension will reduce both the tensile strength and the stiffness (He et al., 2006). In addition, it has been shown that the anisotropy is responsible for the discrepancy between compression and tension strength (Desmorat, 2004; Desmorat, 2006).

Because of the coupling between elasticity and damage, if a straight forward extension of isotropic damage theory to anisotropy case is made, the damage variable is represented by a fourth order tensor (Krajcinovic, 1985; Chaboche, 1979; Leckie and Onat, 1981; Lemaitre and Chaboche,1987) for the case of general anisotropy. This simple method is not our choice because there will have too many material parameters introduced. Considering the physical interpretation of damage in cement-based materials and the efficiency of the model, we use a second order damage tensor (Cordebois and Sidoroff, 1982; Ladevèze, 1983; Chow and Wang, 1987Murakami, 1988) in this paper to deal with concrete.

In this study, a new and more suitable state potential is proposed in order to adequately describe concrete behaviors under tension and compression. The principle of strain equivalence i.e., assuming that the strains in both the effective (undamaged) and damaged configurations are equal is used in deriving the coupled elastic-damage model. A thermodynamic framework for concrete anisotropic damage model is then presented, in which strain mechanisms are identified. Each variable is physically explained and justified. In addition, a numerical scheme is introduced and some numerical examples are presented. Finally, correlative experiments were carried out to validate the capability and accuracy of the proposed constitutive model.

2 AIMS AND SCOPE OF RESEARCH

In the framework of this study, damage of structural concrete was estimated combining CDM with correlative experiments. The nonlinear deformation behaviors under uni-axial, bi-axial and tri-axial loadings were quantitatively analyzed. Afterwards, the damage was quantitatively defined by CDM. This research is aimed at predicting the behaviors of concrete under uni-axial compression, tension and multi-axial loadings so that to obtain an accurate modeling of concrete behaviors which could be used in the nonlinear finite element analysis of the large-scale concrete structures. In addition, this work is benefit to bringing an easy understanding of damage mechanism in concrete structures which are usually subjected to severe dangerous effects like earthquake, wind, environmental, etc., decreasing the life of a structure.

3 THERMODYNAMICALLY BASED CONSTITUTIVE EQUATIONS

3.1 STATE POTENTIAL

The thermodynamics framework proposed by Ladevèze (1983) leading to 3D continuous stress–strain responses is used (Lemaitre and Desmorat, 2005; Desmorat et al., 2007). In their theory, the Helmholtz elastic potential is split into its deviatoric part affected by a tensorial damage variable $\mathbf{D}$ and its hydrostatic part affected by another (scalar) damage variable D_H.

$$\rho\psi^* = \frac{(1-2\nu)}{6E}\frac{\mathrm{tr}(\boldsymbol{\sigma})^2}{1\text{-}\eta D_H} + \frac{1+\nu}{2E}\mathrm{tr}(\mathbf{H}\boldsymbol{\sigma}^D\mathbf{H}\boldsymbol{\sigma}^D) \tag{1}$$

where E, ν represent the Young modulus and Poisson ratio of initially isotropic elasticity respectively, η means the hydrostatic sensitivity parameter (η=3 for most materials [40]), ρ

stands the concrete density, $\boldsymbol{\sigma}^D$ is the deviatoric stress tensor, $\mathbf{H}$ is the effective damage tensor and D_H is the hydrostatic damage.

$$\boldsymbol{\sigma}^D = \boldsymbol{\sigma} - \frac{1}{3}\mathrm{tr}(\boldsymbol{\sigma}), \mathbf{H} = (\mathbf{I}-\mathbf{D})^{-\frac{1}{2}} \text{ and } D_H = \frac{1}{3}\mathrm{tr}\mathbf{D} \tag{2}$$

where $(\mathbf{I}-\mathbf{D})^{-\frac{1}{2}}$ is gained from its diagonal form $(\mathbf{I}-\mathbf{D})_{diag}, (\mathbf{I}-\mathbf{D})_{diag} = \mathbf{P}^{-1}(\mathbf{I}-\mathbf{D})\mathbf{P}$, $(\mathbf{I}-\mathbf{D})^{-1/2} = \mathbf{P}(\mathbf{I}-\mathbf{D})_{diag}^{-1/2}\mathbf{P}^{-1}$, $\mathbf{I} = \delta_{ij}$ is the identity tensor and $\mathbf{P}$ is the coordinate transformation matrix formed by unit eigenvectors of $(\mathbf{I}-\mathbf{D})$.

In their work, whatever hydrostatic stress is positive or negative (positive value represents hydrostatic tension, vice versa), hydrostatic stress is affected by hydrostatic damage at the same degree. Inspired by quasi-brittle materials such as concrete exhibit a strong difference of behavior in tension and in compression due to damage and partial closure effect (Ortiz, 1985; Chaboche, 1993; Murakami and Kamiya, 1997; Halm and Dragon, 1998), we consider there are different impacts on the positive and negative hydrostatic stress coupling with hydrostatic damage. So thermodynamics potential can be developed as follows

$$\rho\psi^* = \frac{(1-2\nu)}{6E}\left[\frac{\langle \mathrm{tr}(\boldsymbol{\sigma})\rangle_+^2}{1-\eta_1 D_H} + \frac{\langle \mathrm{tr}(\boldsymbol{\sigma})\rangle_-^2}{1-\eta_2 D_H}\right] + \frac{1+\nu}{2E}\mathrm{tr}(\mathbf{H}\boldsymbol{\sigma}^D\mathbf{H}\boldsymbol{\sigma}^D) \tag{3}$$

where the notation $\langle\bullet\rangle_+$ stands for the positive part of a scalar, $\langle x\rangle_+ = \max(0,x)$, and $\langle\bullet\rangle_-$ stands for the negative part of a scalar, $\langle x\rangle_- = \min(0,x)$.

The state laws are obtained by derivation of the potential with respect to the thermodynamics variables. The elasticity law coupled with anisotropic damage reads:

$$\boldsymbol{\varepsilon} = \rho\frac{\partial\psi^*}{\partial\boldsymbol{\sigma}} = \frac{(1-2\nu)}{3E}\left[\frac{\langle \mathrm{tr}(\boldsymbol{\sigma})\rangle_+}{1-\eta_1 D_H} + \frac{\langle \mathrm{tr}(\boldsymbol{\sigma})\rangle_-}{1-\eta_2 D_H}\right]\mathbf{I} + \frac{1+\nu}{E}(\mathbf{H}\boldsymbol{\sigma}^D\mathbf{H})^D \tag{4}$$

where $\mathbf{I}$ is the identity tensor. Actually, it also produce secant operator presented in appendix **A**. If uni-axial tension is applied in direction 1 (see Figure 1), the elastic strains in this frame are

$$\begin{bmatrix} \varepsilon_1^e & & \\ & \varepsilon_2^e & \\ & & \varepsilon_3^e \end{bmatrix} = \frac{1-2\nu}{3E}\frac{\sigma_1}{1-\eta_1 D_H}\begin{bmatrix} 1 & & \\ & 1 & \\ & & 1 \end{bmatrix} + \frac{1+\upsilon}{E}\left(\begin{bmatrix} \frac{1}{\sqrt{1-D_1}} & & \\ & \frac{1}{\sqrt{1-D_2}} & \\ & & \frac{1}{\sqrt{1-D_3}} \end{bmatrix}\begin{bmatrix} \frac{2\sigma_1}{3} & & \\ & \frac{-\sigma_1}{3} & \\ & & \frac{-\sigma_1}{3} \end{bmatrix}\begin{bmatrix} \frac{1}{\sqrt{1-D_1}} & & \\ & \frac{1}{\sqrt{1-D_2}} & \\ & & \frac{1}{\sqrt{1-D_3}} \end{bmatrix}\right)^D \tag{1}$$

The decoupling between the deviatoric and the volumic part of the stress-strain relation induces only a partial stiffness recovery sufficient for monotonic applications. In tension the dam-

aged bulk modulus is $\overline{K} = (1-\eta_1 D_H)K$. Note that the shear-bulk coupling is nevertheless represented. The trace of damage $\mathbf{D}$ acts on the hydrostatic stress.

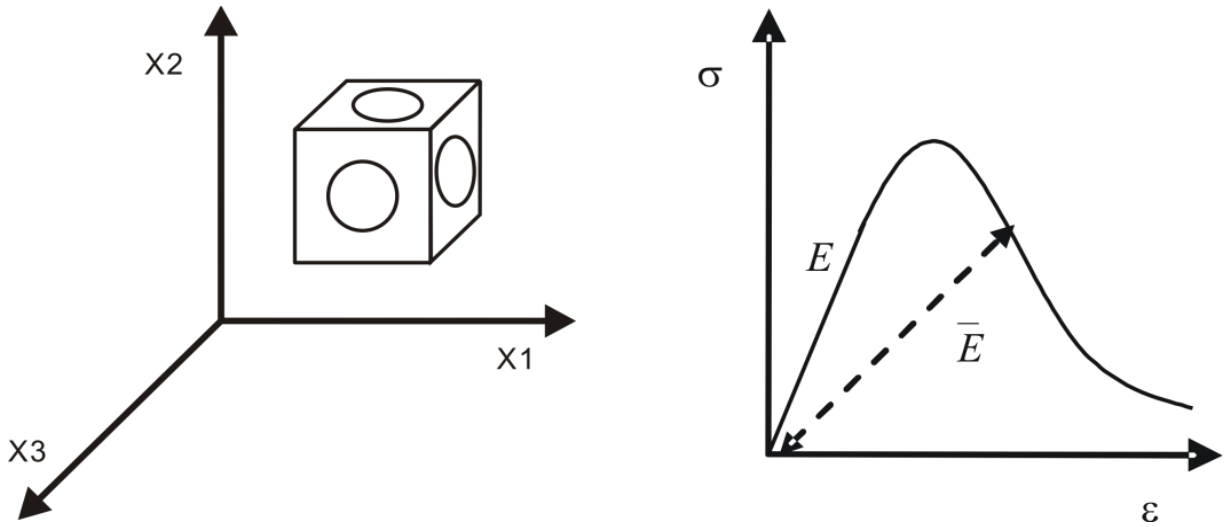

Figure 1. Damaged elasticity in the principal direction

Consider a representative volume element (RVE) damaged in the orthotropic frame $(\vec{x}_1, \vec{x}_2, \vec{x}_3)$ of Figure1

$$\mathbf{D} = \begin{bmatrix} D_1 & & \\ & D_2 & \\ & & D_3 \end{bmatrix} \tag{6}$$

If the three principal stresses are of the same sign, from equation (4) the elasticity law reads

$$\boldsymbol{\varepsilon} = \left[\mathbf{B}(D_1, D_2, D_3) \frac{1}{E} \right] \boldsymbol{\sigma} \tag{7}$$

where $\mathbf{B}$ is a tensor presented in appendix $\mathbf{B}$ in details. If a tension loading is applied in the direction X_1, $\mathbf{B}$ can be rewritten as follows

$$\begin{aligned} B_{11} &= \frac{E}{\overline{E}_1}, B_{12} = B_{21} = \bar{\nu}_{12} \frac{E}{\overline{E}_1}, B_{13} = B_{31} = \bar{\nu}_{13} \frac{E}{\overline{E}_1}, \\ B_{22} &= \frac{E}{\overline{E}_2}, B_{23} = B_{32} = \bar{\nu}_{23} \frac{E}{\overline{E}_2}, B_{33} = \frac{E}{\overline{E}_3}, \end{aligned} \tag{8}$$

where $\overline{E}_i$ is the damaged modulus in i direction. So if together with appendix $\mathbf{B}$, the measurement of the uni-axial stress-strain relation gives a possibility to measure the damage. Practically, most of the time, it is not possible to obtain three specimens in three orthogonal directions but

four measures are sufficient if the orthotropic directions are known. In the case of a damaged plane sheet, the only possible directions for measures are $\mathbf{X}_1$ and $\mathbf{X}_2$ to give $\overline{E}_1$, $\overline{E}_2$ and $\overline{\nu}_{12}$ then

$$D_1 = 1 - \frac{\overline{E}_1}{E}(1+\nu)(2+\overline{\nu}_{12} - \frac{\overline{E}_1}{\overline{E}_2})^{-1}$$
$$D_2 = 1 - \frac{\overline{E}_2}{E}(1+\nu)[2-(1-\overline{\nu}_{12})\frac{\overline{E}_2}{\overline{E}_1}]^{-1} \tag{9}$$
$$\eta D_H = 1 - \frac{\overline{E}_1}{E}\frac{1-2\nu}{1-2\overline{\nu}_{12}}$$

With the help of strain equivalence principle, previous elasticity law can be rewritten as $\overline{\boldsymbol{\sigma}} = \mathbf{C} : \boldsymbol{\varepsilon}$ or $\boldsymbol{\varepsilon} = \mathbf{C}^{-1} : \overline{\boldsymbol{\sigma}} = \frac{1+\nu}{E}\overline{\boldsymbol{\sigma}} - \frac{\nu}{E}\mathrm{tr}(\overline{\boldsymbol{\sigma}})\mathbf{I}$, where $\mathbf{C}$ is forth tensor. This defines analytically the relationship between the Cauchy stress $\boldsymbol{\sigma}$ and the effective stress $\overline{\boldsymbol{\sigma}}$, which is symmetric and independent from the elasticity parameters,

$$\overline{\boldsymbol{\sigma}} = \frac{1}{3}[\frac{\langle \mathrm{tr}(\boldsymbol{\sigma})\rangle_+}{1-\eta_1 D_H} + \frac{\langle \mathrm{tr}(\boldsymbol{\sigma})\rangle_-}{1-\eta_2 D_H}]\mathbf{I} + [(\mathbf{H}\boldsymbol{\sigma}^D\mathbf{H}\boldsymbol{\sigma}^D)]^D \tag{10}$$

At the same time, Cauchy stress can be replaced by

$$\boldsymbol{\sigma} = (\mathbf{I}-\mathbf{D})^{1/2}\overline{\boldsymbol{\sigma}}(\mathbf{I}-\mathbf{D})^{1/2} - \frac{(\mathbf{I}-\mathbf{D}):\overline{\boldsymbol{\sigma}}}{3-\mathrm{tr}\mathbf{D}}(\mathbf{I}-\mathbf{D}) + \frac{1}{3}[(1-\mathrm{tr}\mathbf{D})\langle \mathrm{tr}\overline{\boldsymbol{\sigma}}\rangle_+ + (1-\frac{\eta_2}{3}\mathrm{tr}\mathbf{D})\langle \mathrm{tr}\overline{\boldsymbol{\sigma}}\rangle_-]\mathbf{I} \tag{11}$$

3.2 Damage threshold and evolution laws

Damage evolution is linked to the reach or not of a threshold. Depending on the materials, the damage threshold may be expressed by strains (Mazars, 1984; Herrmann and Kestin, 1988; Ramtani,1990; Devree et al., 1995; Geers et al., 2000), stresses (Ortiz, 1985; Warnke, 1975) or damage energy release rate (Marigo, 1985; Laborderie,1990). The most efficient way to express constitutive equations arguing for straightforward numerical integration is to make use of a damage threshold based on strains. For brittle materials like concrete, Mazars's criterion defining an equivalent strain ε_{eq} is here used for the anisotropic growth of damage. The equivalent strain ε_{eq} is built from the positive principal strain ε_{I} (the extensions)

$$\varepsilon_{eq} = \sqrt{\langle\boldsymbol{\varepsilon}\rangle_+ : \langle\boldsymbol{\varepsilon}\rangle_+} = \sqrt{\sum \langle\boldsymbol{\varepsilon}_{\mathrm{I}}\rangle_+^2} \tag{12}$$

The damage threshold takes the simple form

$$f = \varepsilon_{eq} - \kappa(\mathrm{tr}\mathbf{D}) \le 0 \tag{13}$$

and

$$\kappa(\mathrm{tr}\mathbf{D}) = a\tan[\frac{\mathrm{tr}\mathbf{D}}{aA} + \arctan(\frac{\kappa_0}{a})] \tag{14}$$

where $f<0$ corresponds to the elasticity domain, $f=0$ and $\dot{f}=0$ correspond to damage growth (consistency condition). $\kappa(\mathrm{tr}\mathbf{D})$ is the consolidation function in the strains space, depending on the trace of the damage tensor. The initial value of $\kappa(\mathrm{tr}\mathbf{D})$ is defined by $\kappa_0=\kappa(0)$.

The identification of different behaviors is performed by the definition of the consolidation function $\kappa(\mathrm{tr}\mathbf{D})$. For concrete, a simple expression has been found which fits the concrete responses in both tension and compression, introducing only two damage parameters a and A in addition to the Young modulus E, the Poisson ratio ν and the damage threshold $\kappa_0=\kappa(0)$.

Within the thermodynamics framework, the corresponding choice for the non-associated potential is

$$F=F(\mathbf{Y};\boldsymbol{\varepsilon})=\mathbf{Y}:\langle\boldsymbol{\varepsilon}\rangle_+^{\beta} \tag{15}$$

and so

$$\dot{\mathbf{D}}=\dot{\lambda}\frac{\partial F}{\partial \mathbf{Y}}=\dot{\lambda}\langle\boldsymbol{\varepsilon}\rangle_+^{\beta}\rightarrow \mathrm{tr}(\dot{\mathbf{D}})=\dot{\lambda}\,\mathrm{tr}(\langle\boldsymbol{\varepsilon}\rangle_+^{\beta}) \tag{16}$$

The damage multiplier is determined from the consistency condition $f=0$ and $\dot{f}=0$.

$$\mathrm{tr}\mathbf{D}=\kappa^{-1}(\varepsilon_{eq}) \text{ and } \mathrm{tr}(\dot{\mathbf{D}})=\frac{\kappa^{-1}(\varepsilon_{eq})}{d\varepsilon_{eq}}\dot{\varepsilon}_{eq} \tag{17}$$

then

$$\dot{\lambda}=\frac{\mathrm{tr}(\mathbf{D})}{\mathrm{tr}(\langle\boldsymbol{\varepsilon}\rangle_+^{\beta})}=\frac{d[\kappa^{-1}(\varepsilon_{eq})]}{d\varepsilon_{eq}}\frac{\dot{\varepsilon}_{eq}}{\mathrm{tr}(\langle\boldsymbol{\varepsilon}\rangle_+^{\beta})} \tag{18}$$

and

$$\dot{\mathbf{D}}=\frac{\mathrm{tr}(\mathbf{D})}{\mathrm{tr}(\langle\boldsymbol{\varepsilon}\rangle_+^{\beta})}\langle\boldsymbol{\varepsilon}\rangle_+^{\beta}=\frac{d(\kappa^{-1}(\varepsilon_{eq}))}{d\varepsilon_{eq}}\frac{\dot{\varepsilon}_{eq}}{\mathrm{tr}(\langle\boldsymbol{\varepsilon}\rangle_+^{\beta})}\langle\boldsymbol{\varepsilon}\rangle_+^{\beta} \tag{19}$$

The exponent β mainly plays a role in multi-axial states of stresses, and setting $\beta=2$ (so that $\mathrm{tr}(\langle\boldsymbol{\varepsilon}\rangle_+^{\beta})=(\varepsilon_{eq})^2$) to make the equivalent strain ε_{eq} appear. This choice is then consistent with Mazars criterion, the damage law simplifying as

$$\dot{D}=\frac{\kappa^{-1}(\varepsilon_{eq})}{d\varepsilon_{eq}}\frac{\dot{\varepsilon}_{eq}}{\varepsilon_{eq}^{\,2}}\langle\boldsymbol{\varepsilon}\rangle_+^{2} \tag{20}$$

Therefore, for concrete, the damage pattern is different in tension and in compression.

When uni-axial tension is applied in direction $\mathbf{X}_1$

$$\langle \boldsymbol{\varepsilon} \rangle_+ = \begin{bmatrix} \varepsilon_1 & 0 & 0 \\ 0 & 0 & 0 \\ 0 & 0 & 0 \end{bmatrix}, \langle \boldsymbol{\varepsilon} \rangle_+^2 = \begin{bmatrix} \varepsilon_1^2 & 0 & 0 \\ 0 & 0 & 0 \\ 0 & 0 & 0 \end{bmatrix} \tag{21}$$

the damage tensor will be

$$\mathbf{D} \approx \begin{bmatrix} D_1 & 0 & 0 \\ 0 & 0 & 0 \\ 0 & 0 & 0 \end{bmatrix} \tag{22}$$

When uni-axial compression is applied in direction X_1

$$\langle \boldsymbol{\varepsilon} \rangle_+ = \begin{bmatrix} 0 & 0 & 0 \\ 0 & \varepsilon_2 & 0 \\ 0 & 0 & \varepsilon_2 \end{bmatrix}, \langle \boldsymbol{\varepsilon} \rangle_+^2 = \begin{bmatrix} 0 & 0 & 0 \\ 0 & \varepsilon_2^2 & 0 \\ 0 & 0 & \varepsilon_2^2 \end{bmatrix} \tag{23}$$

the damage tensor will be

$$\mathbf{D} \approx \begin{bmatrix} 0 & 0 & 0 \\ 0 & D_2 & 0 \\ 0 & 0 & D_2 \end{bmatrix} \tag{24}$$

3.3 Rupture control with anisotropic damage

Describing rupture of structural, it needs to deal with elements at high levels of damage, the ultimate state of degradation corresponding to eigenvalues of damage tensor close to unity. The damage acts by its individual values on the deviatoric part of the behavior and by its trace on the volumic part. It is obvious that one has to consider two different treatments for the damage evolution, depending on which part of the behavior is concerned. Such a treatment must simply ensure that the effective damaged elasticity tensor $\overline{E}$ remains positive definite.

Concerning the hydrostatic part of the constitutive equations, the limitations at high level of damage appears clearly when observing the reversible process equations.

$$\mathrm{tr}\boldsymbol{\varepsilon} = \frac{\langle \mathrm{tr}\boldsymbol{\sigma} \rangle_+}{3K(1-\frac{\eta_1}{3}\mathrm{tr}\mathbf{D})} + \frac{\langle \mathrm{tr}\boldsymbol{\sigma} \rangle_-}{3K(1-\frac{\eta_2}{3}\mathrm{tr}\mathbf{D})} \tag{25}$$

with K the bulk modulus of the virgin (isotropic) material. There are situations such as compression leading to $\mathrm{tr}\mathbf{D} > 1$. These are admissible as long as they are mainly compressive, more precisely as long as $\mathrm{tr}\boldsymbol{\sigma} < 0$,as the hydrostatic stiffness remains equal to $3K$ .But they become critical

when a change in the loading sign occurs if the broken material behavior is not properly defined as then $3K(1-\mathrm{tr}\mathbf{D})$ is negative and cannot therefore act as a material stiffness. The physical meaning of a large damage trace due to compression is that the material highly damaged, still resist for compressive states of stresses but will be broken in pieces as soon as tensile stresses are applied on it. It is possible to continue the computation by defining a fictitious hydrostatic broken behavior for the material such as

$$\mathrm{tr}\boldsymbol{\varepsilon} = \frac{\langle \mathrm{tr}\boldsymbol{\sigma} \rangle_+}{3\overline{K}_1} + \frac{\langle \mathrm{tr}\boldsymbol{\sigma} \rangle_-}{3\overline{K}_2} \tag{26}$$

where if $\frac{\eta_1}{3}\mathrm{tr}\mathbf{D} \le D_c$

$$\overline{K}_1 = K(1-\frac{\eta_1}{3}\mathrm{tr}\mathbf{D}), \overline{K}_2 = K(1-\frac{\eta_2}{3}\mathrm{tr}\mathbf{D}) \tag{27}$$

if $\frac{3D_c}{\eta_2} \ge \frac{\eta_1}{3}\mathrm{tr}\mathbf{D} \ge D_c$

$$\overline{K}_1 = K(1-D_c), \overline{K}_2 = K(1-\frac{\eta_2}{3}D_c) \tag{28}$$

and if $\mathrm{tr}\mathbf{D} \ge \frac{3D_c}{\eta_2}$

$$\overline{K}_1 = K(1-D_c), \overline{K}_2 = K(1-D_c) \tag{29}$$

For the deviatoric case, to ensure that the damaged elasticity operator remains positive definite, one only has to impose that the eigenvalues of the second order damage tensor are bounded by 1, or by D_c from a numerical point of view (Lemaitre et al., 2000; Badel et al., 2007). Under these conditions, the general damage law $\dot{\mathbf{D}} = \dot{\lambda}\langle\boldsymbol{\varepsilon}\rangle_+^2$ needs an adaptation. If the maximum eigenvalue of damage $D_{\mathrm{I}}(D_{\mathrm{I}} > D_{\mathrm{II}} > D_{\mathrm{III}})$ reaches its critical value D_c in n_{I} direction, damage growth in that direction stops and fracture occurs, defining a first plane of fixed crack in the solid. Later on damage grows in the remaining $(n_{\mathrm{II}}, n_{\mathrm{III}})$ directions. The damage evolution law is kept unchanged in terms of the (2D) strain tensor in the $(n_{\mathrm{II}}, n_{\mathrm{III}})$ plane, keeping $D_{\mathrm{I}} = D_c$ along n_{I} direction. If loading continues, the second direction, in which the damage reaches its critical value, is also detected, defining the plane of crack in a similar fashion. The third direction is oriented orthogonal to the first two directions. Three families of cracks are, therefore, introduced at the peak stage that finally led the test specimen to complete fracture and the final behavior resulted (with different bulk modulus in tension and in compression)

$$\boldsymbol{\sigma} = 2G(1-D_c)\boldsymbol{\varepsilon}^D + K[(1-D_c)\langle \mathrm{tr}\boldsymbol{\varepsilon}\rangle_+ + (1-D_c)\langle \mathrm{tr}\boldsymbol{\varepsilon}\rangle_-]\mathbf{I} \tag{30}$$

where $G = E/2(1+\nu)$ is the shear modulus.

4 Numerical Implantation

4.1 Euler backward scheme

The major advantage of this model is its easy numerical implementation within any finite element code and its corresponding robustness regarding computations at the structural scale. Euler backward scheme is used, i.e. the variables are replaced by their value at time in the constitutive equations when the damage rate and the damage multiplier are replaced by and in the damage law. In order to integrate the damage model proceed as follows:

1- Compute the equivalent strain,

$$\varepsilon_{eq(n+1)} = \sqrt{\langle \boldsymbol{\varepsilon}_{n+1}\rangle_+ : \langle \boldsymbol{\varepsilon}_{n+1}\rangle_+} \tag{30}$$

2- Calculate the threshold function trial: $f_{trial} = \varepsilon_{eq(n+1)} - \kappa(\mathrm{tr}\mathbf{D}_n)$ with equivalent strain. If $f \le 0$, the damage does not evolve, $\mathbf{D}_{n+1} = \mathbf{D}_n$. Else if $f > 0$, the damage must be corrected by using the damage evolution law described as (setting $\beta = 2$),

$$\begin{cases} \Delta\mathbf{D} = \mathbf{D}_{n+1} - \mathbf{D}_n = \Delta\lambda \langle \boldsymbol{\varepsilon}_{n+1}\rangle_+^2 \\ \Delta\lambda = \dfrac{\mathrm{tr}\mathbf{D}_{n+1} - \mathrm{tr}\mathbf{D}_n}{\varepsilon_{eq(n+1)}^2} \end{cases} \tag{31}$$

Then update the damage tensor $\mathbf{D}$, $\mathbf{D}_{n+1} = \mathbf{D}_n + \Delta\lambda \langle \boldsymbol{\varepsilon}_{n+1}\rangle_+^2$

3- Compute the effective stresses: $\bar{\boldsymbol{\sigma}}_{n+1} = \mathbf{C} : \boldsymbol{\varepsilon}_{n+1}$

4- Determine the Cauchy stresses:

$$\begin{aligned} \boldsymbol{\sigma}_{n+1} = {} & (\mathbf{I}-\mathbf{D}_{n+1})^{1/2}\bar{\sigma}_{n+1}(\mathbf{I}-\mathbf{D}_{n+1})^{1/2} - \frac{(\mathbf{I}-\mathbf{D}_{n+1}):\bar{\boldsymbol{\sigma}}_{n+1}}{3-\mathrm{tr}(\mathbf{D}_{n+1})}(\mathbf{I}-\mathbf{D}_{n+1}) \\ & + \frac{1}{3}[(1-\mathrm{tr}\mathbf{D}_{n+1})\langle \mathrm{tr}\bar{\boldsymbol{\sigma}}_{n+1}\rangle_+ + (1-\frac{\eta_2}{3}\mathrm{tr}\mathbf{D}_{n+1})\langle \mathrm{tr}\bar{\boldsymbol{\sigma}}_{n+1}\rangle_-]\mathbf{I} \end{aligned} \tag{32}$$

At the end, a program code was prepared in MATLAB 7.11 to implement the algorithm. Additionally, the constitutive law of elements was derived and adopted; no meshing technique was used.

4.2 Experiments and numerical results

4.2.1 Raw materials and preparation of specimens

Cement used in this study was ASTM Type I Portland cement (or Ordinary Portland Cement in

BSI), with relative density of 3.15 and fineness of $385\mathrm{m}^2/\mathrm{kg}$. The average particle size for cement is $19.98\,\mu\mathrm{m}$. The coarse aggregate used was crushed limestone with maximum size of 10 mm, and relative density of 2.57. The fine aggregate used was natural river sand with a fineness modulus of 2.3, and relative density of 2.66. The mix proportion for normal concrete by weight was, cement : water : sand : coarse aggregate = 1.0 : 0.5 : 1.5 : 2.4. The concretes were mixed with a pan mixer following the procedures recommended by ASTMC192-M. After mixing, a vibrating table was used to ensure a good compaction. The surface of the concrete was then smoothed and a wet cloth was used to cover the concrete until the specimens were demolded for testing or further curing one day after casting. The further curing of demolded specimens were carried out in a curing room with a temperature of $21\pm2°\mathrm{C}$.

4.2.2 Uni-axial compression

A complete stress-strain curve represents a comprehensive response of concrete to external force. It can reflect the influence of damage process, microcrack development including random occurrence and localization, and formation and propagation of major crack on a global scale.

Compressive tests were carried out using three cylindrical specimens. The modulus of elasticity and complete stress-strain curve were measured using a digital closed-loop controlled MTS machine with a capacity of 450 metric tons (Model 815). The tests were carried out using the circumferential control by putting a roller chain on specimen in a transverse direction (Jin and Li, 2000).

The tests were initially controlled by a loading rate of 1.5 kN/sec, and then transferred to a circumferential deformation control of 0.0008 mm/sec. Complete stress-strain curves can be easily obtained by using such a control method.

The comparison of uni-axial tensile stress-strain curves between experiment and numerical results is shown in Figure 2. At the same time, strain-damage curve is obtained. The material parameters used in the analysis are $E=24\mathrm{GPa}, \nu=0.2,\ \eta_1=3, \eta_2=0.5,\ a=2.88605\mathrm{e}-4,$ $A=7.7\mathrm{e}3,\ k_0=1.35\mathrm{e}-4,$ where E and ν were obtained from experiments, while $\eta_1, \eta_2, a, A, k_0$ were taken for different materials and from reference (Desmorat et al., 2007).

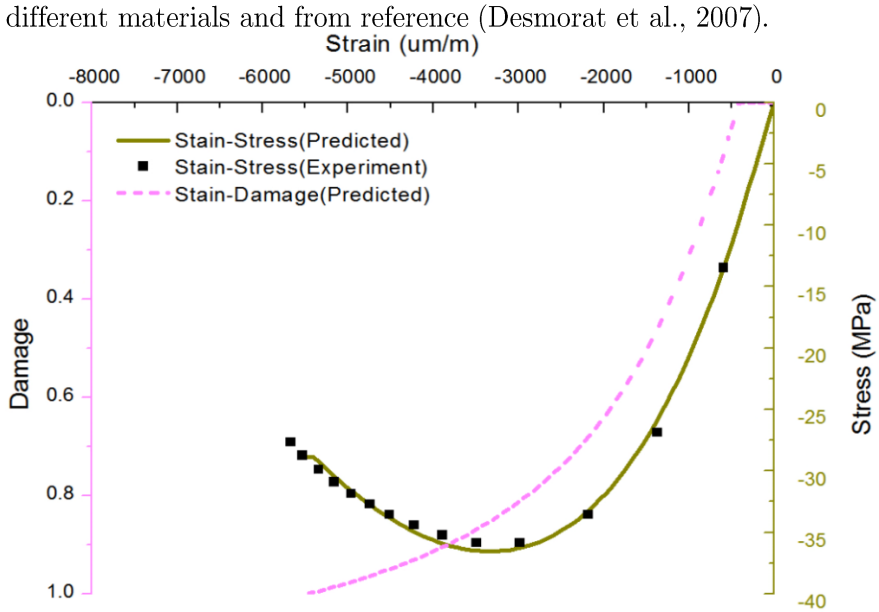

Figure 2. Strain curves for concrete applied in uni-axial compression ($E=24\mathrm{MPa}, \nu=0.2$)

4.2.3 Uni-axial tension

Compared to the compressive behavior of concrete, its tensile behavior has received a little attention in the past, partly because it is a common practice to ignore tensile resistance in reinforced concrete design. Interest in tensile properties has grown substantially in recent years partially due to introduction of fracture mechanics into the field of concrete structures. In addition, the tensile strength of concrete is important to resist cracking from shrinkage and temperature changes. However, available information on the complete stress-deformation curve of plain concrete under uni-axial tension is scarce, especially for un-notched concrete specimens. This is mainly due to the control difficulties in direct uni-axial tension tests. By applying a recently developed adaptive control method, this research has success fully obtained the complete stress deformation curves for un-notched concrete specimens under uni-axial tension. These results provide rational information on nature of tension behavior of young concrete, including the process of internal damage.

The tension specimens were cast in a premade acrylic glass mold with the dimension of 350×100×20 mm. The mold was made of acrylic sheet with a thickness of 25 mm. With such a specimen size, the uni-axial tension can be ensured as a two-dimensional problem and a total of 12 plate specimens were prepared.

Uni-axial tension tests were conducted using a newly developed test method (Figure 3). Several measures have been taken to ensure a success of uni-axial tension test. To avoid possible eccentricity or bending of the tension specimen, a set of special loading fixture was developed (Tension strength in experiment is 3.21MPa).

Constitution relation between stress and strain under uni-axial tensile loading is presented in Figure 4 (Tension strength in experiment is 3.21MPa). One can observe that with only one thermodynamic variable (the damage tensor),and the model is able to correctly describe the non-symmetric uni-axial behavior of concrete.

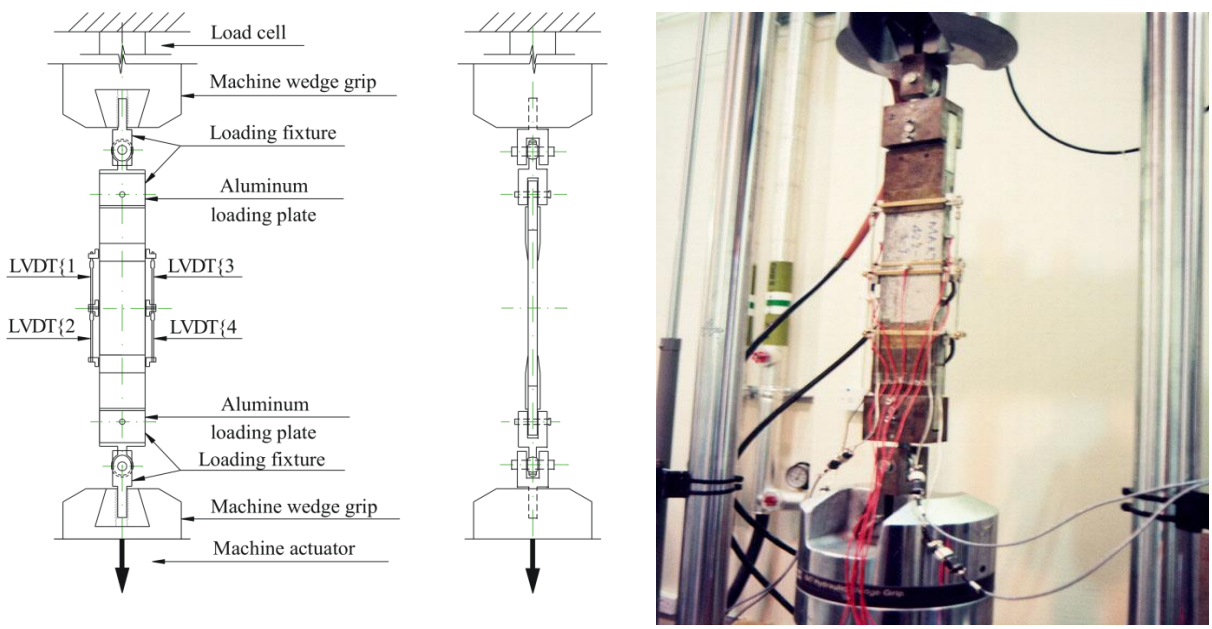

Figure 3. Uni-axial tension test setup

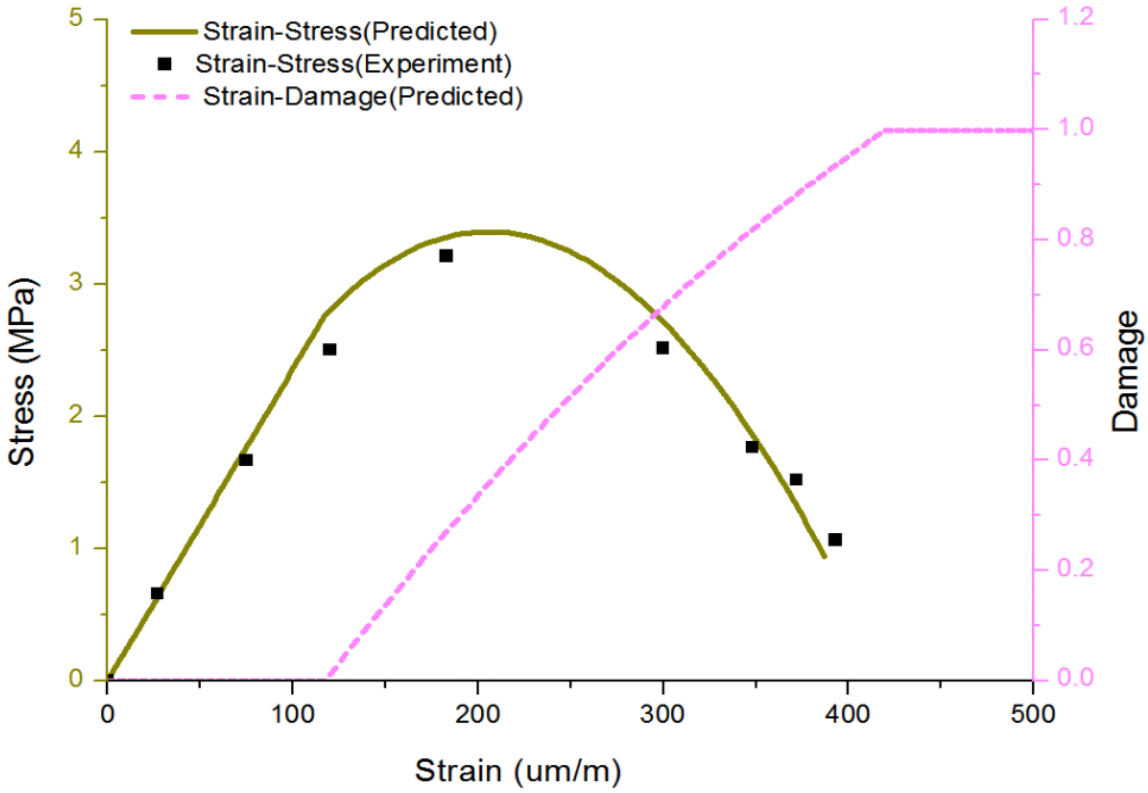

Figure 4. Strain curves for concrete applied in uni-axial tension

4.2.4 Multi-axial numerical results

Using the same material parameters as above, the numerical result of bi-axial compression is obtained in Figure 5. The stress introduced in Figure 5 was in the direction of applied compression load. Since the load application to the test specimen was done in multi-axial directions, the compression loading application possesses two directions. In the third direction, because of Possion's effect, tensile strains occurred. Hence the direction of damage depicted in Fig. 5 was the third direction. Obviously, compressive strength of the bi-axial compression is higher than that of the uni-axial compression. Moreover, the concrete under bi-axial compression performs more brittle than uni-axial compression. As for comparing with the uni-axial compression, whose evolution of damage is in two principal directions, cracks under bi-axial compression are propagated just in one principal direction. Moreover, the response of concrete applied in tri-axial tension is shown in Figure 6. Because the initiation and propagation of cracks in concrete is developed rapidly in three principal directions, the concrete provides most low strength under tri-axial tension.

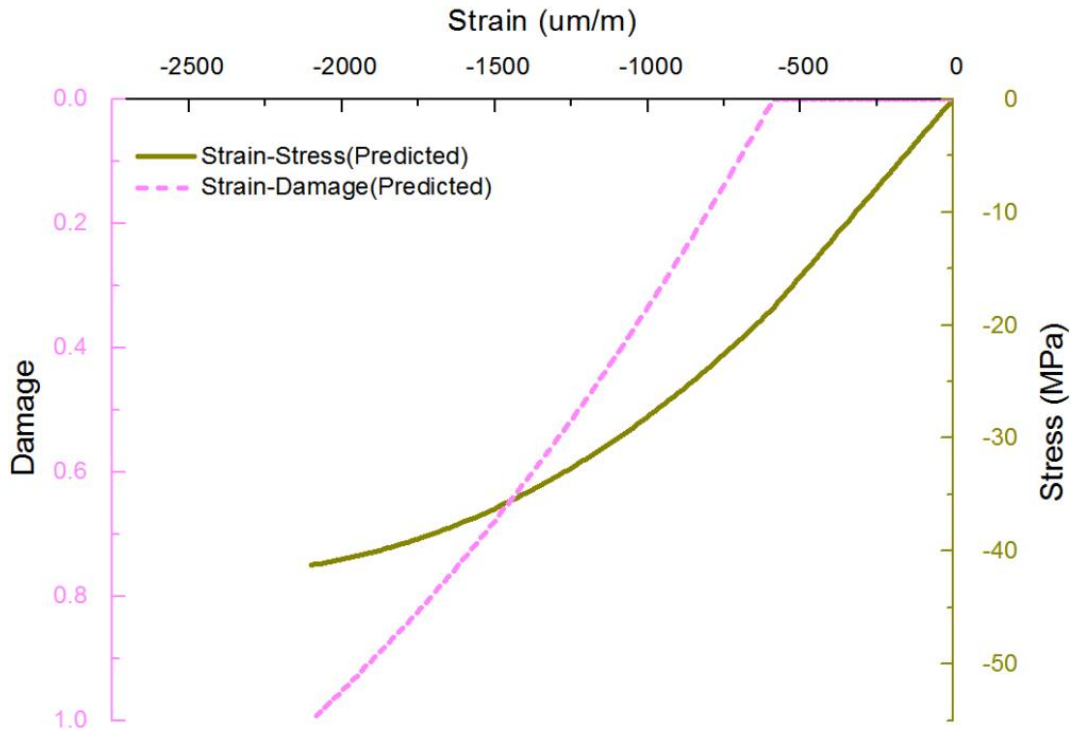

Figure 5. Strain curves for concrete applied in bi-axial compression

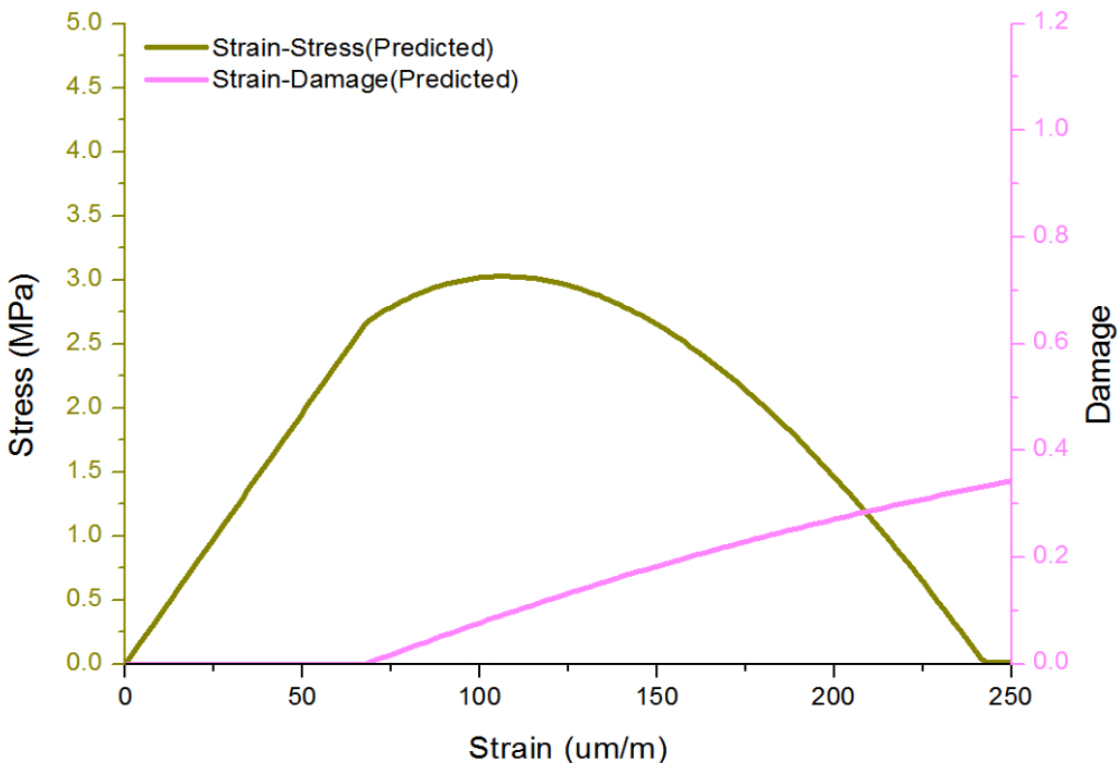

Figure 6. Strain curves for concrete applied in tri-axial tension

As stated earlier, in this research the constitutive law of elements was derived and used to measure the variables, while the mesh and nodal approach was not followed. Our work is a preliminary work of finite element analysis. The outcomes of this work if adopted, as is proposed in our study, can be very useful in applying the multi-axial stress-strain relationship to analyze the large scale structures.

5 CONCLUSIONS

In this paper, with the help of CDM, a new suitable state potential is proposed for concrete in order to express the state equations for modeling the special mechanical behaviors. The damage state corresponds to a given micro-cracks pattern and, accordingly to the definition of thermodynamics state variables, it is represented by a single second-order tensor damage variable **D** whatever the sign of the loading. The strong dissymmetry of concrete behaviors is represented and is shown to be mainly due to induced damage anisotropy. Based on strain equivalence method, a new constitution model is deducted in this paper. A numerical scheme is introduced and some numerical examples are presented. Experiments were carried out in order to validate the capability of the proposed model. In a word, the model can get the unilateral effect and multi-axial effect of concrete correctly. The outcomes of this research will bring an easy understanding of concrete material behavior under uni-axial compression, tension and multi-axial loadings. It will be very useful in nonlinear finite element analysis of the large-scale concrete structures.

Acknowledgements

The financial supports from National Basic Research Program of China (973 Program) (Grant No. 2009CB623200), Chinese Natural Science Foundation (Grant No. 50838008 and 511784130) and the Alexander von Humboldt (AvH) Foundation of Germany are greatly acknowledged.

References

A.A. Shah and Hirose S. Nonlinear ultrasonic investigation of concrete damaged under uniaxial compression step loading. *ASCE Journal of Materials in Civil Engineering*, 22(5):476–84,2010.

A.A. Shah, S.H. Alsayed, H. Abbas and Y.A. Al-Salloum. Predicting residual strength of non-linear ultrasonically evaluated damaged concrete using artificial neural network. *Construction and Building Materials*, 29(1):42–50,2012.

J. Mazars. A description of micro-and macroscale damage of concrete structures. *Eng Fract Mech.*, 25:729-37, 1986.

C. Poinard, Y. Malecot and L. Daudeville. Damage of concrete in a very high stress state: experimental investigation. *Mater Struct.*, 43:15-29, 2010.

B. Richard, F. Ragueneau, C. Cremona and L. Adelaide. Isotropic continuum damage mechanics for concrete under cyclic loading: Stiffness recovery, inelastic strains and frictional sliding. *Eng Fract Mech.*, 77:1203-23, 2010.

A.C.T. Chen and W.F. Chen. Constitutive relations for concrete. *Journal of Engineering Mechanics*, 101: 1975.

Z. Bażant Endochronic inelasticity and incremental plasticity. *Int J Solids Struct.*, 14:691-714, 1978.

A. Dragon and Z. Mroz. A continuum model for plastic-brittle behaviour of rock and concrete. *Int J Eng Sci.*, 17:121-37,1979.

H.L. Schreyer. A third-invariant plasticity theory for frictional materials. *Journal of structural mechanics*, 11:177-96,1983.

E.S. Chen and O. Buyukozturk. Constitutive model for concrete in cyclic compression. *Journal of Engineering Mechanics*, 111:797-814,1985.

E. Onate, S. Oller, J. Oliver and J. Lubliner. A constitutive model for cracking of concrete based on the incremental theory of plasticity. *Engineering Computations: Int J for Computer-Aided Engineering*, 5:309-19,1993.

G.Z. Voyiadjis and T.M.Abulebdeh. Plasticity model for concrete using the bounding surface concept. *Int J Plasticity*, 10:1-21, 1994.

A. Karabinis and P. Kiousis. Effects of confinement on concrete columns: plasticity approach. *Journal of*

structural engineering, 120:2747-67,1994.
P. Menetrey and K.Willam. Tri-axial failure criterion for concrete and its generalization. *ACI Structural Journal*, 92:1995.
P. Grassl, K. Lundgren and K. Gylltoft. Concrete in compression: a plasticity theory with a novel hardening law. *Int J Solids Struct*, 39:5205-23,2002.
M.P. Nielsen. Limit analysis and concrete plasticity. CRC: 2010.
D. Krajcinovic. Continuous damage mechanics revisited - basic concepts and definitions. *J Appl Mech-T Asme*, 52:829-34,1985.
S. Yazdani and H. Schreyer. Combined plasticity and damage mechanics model for plain concrete. *Journal of Engineering Mechanics*, 116:1435-50, 1990.
D. Fanella and D. Krajcinovic. A micromechanical model for concrete in compression. *Eng Fract Mech.*, 29:49-66,1988.
Z.P. Bazant and P.C. Prat. Microplane model for brittle-plastic material: I. Theory. *Journal of Engineering Mechanics*, 114:1672-88,1988.
I. Carol, Z.P. Bazant and P.C. Prat. Geometric damage tensor based on microplane model. *Journal of Engineering Mechanics*, 117:2429-48,1991.
I. Carol, P.C. Prat and Z.P. Bazant. New explicit microplane model for concrete: theoretical aspects and numerical implementation. *Int J Solids Struct.*, 29:1173-91,1992.
J. Mazars and G. Pijaudier-Cabot. Continuum damage theory- Application to concrete. *Journal of Engineering Mechanics*, 115:345-65,1989.
L.M. Kachanov. Time of the rupture process under creep conditions. *Izvestiya Akademii Nauk USSR Otd Tech.*, 8:26-31,1958.
J. Mazars. Application de la mécanique de l'endommagement au comportement non linéaire et à la rupture de béton de structure. France: Université Paris VI: 1984. (in French)
Z.P. Bazant and G. Pijaudier-Cabot. Nonlocal continuum damage, localization instability and convergence. *Journal of Applied Mechanics*, 55:287-93,1988.
J. Lemaitre and H. Lippmann. A course on damage mechanics: *Springer Berlin*, 1996.
W. He, Y.F. Wu, K.M. Liew and Z.S. Wu. A 2D total strain based constitutive model for predicting the behaviors of concrete structures. *Int J Eng Sci.*, 44:1280-303,2006.
R. Desmorat. Modèle d'endommagement anisotrope avec forte dissymétrie traction/compression. *Proceeding of 5è journèees du Regroupement Francophone pour la Recherche et la Formation sur le Bèton (RF2B)*, Liège, Belgium 2004. (in French)
R. Desmorat. Positivity of intrinsic dissipation of a class of nonstandard anisotropic damage models. *Cr Mecanique*, 334:587-92,2006.
J.L. Chaboche. Le concept de contrainte effective applique a lelastieite et la viscoplaticite en presence d'un endommagement anisotrope. *Report Colloq Euromech*, France, 1979. (in French)
F.A. Leckie and E.T. Onat. Tensorial nature of damage measuring internal variables. In: J. H, J. L, editors. Proceedings of IUTAM Symposium: *Physical Non-linearities in Structural Analysis*, Berlin: Springer, 1981.
J. Lemaitre and J.L. Chaboche. Mechanics of Solid Materials. Berlin: Springer, 1987.
S. Murakami and N. Ohno. A constitutive equation of creep damage in pollicristalline metals. Proceedings of IUTAM Colloquium Euromech 111. Marienbad: Springer, 1978.
J. Cordebois and F. Sidoroff. Anisotropic damage in elasticity and plasticity. *J Mec Theor Appl.*, 45-60,1982.
P. Ladevèze. On an anisotropic damage theory. In: Boehler JP, editor. *Proceedings of CNRS Int Coll 351 Villars-de-LansFailure criteria of structured media*, 355-63,1983.
C.L. Chow and J. Wang. An anisotropic theory of elasticity for continuum damage mechanics. *Int J Fracture*, 33:3-16,1987.
S. Murakami. Mechanical modeling of material damage. *J Appl Mech-T ASME*, 55:280-6, 1988.
J. Lemaitre and R. Desmorat. Engineering damage mechanics: ductile, creep, fatigue and brittle failures. Berlin: Springer, 2005.
R. Desmorat, F. Gatuingt and F. Ragueneau. Nonlocal anisotropic damage model and related computational aspects for quasi-brittle materials. *Eng Fract Mech.*, 74:1539-60, 2007.
M. Ortiz. A constitutive theory for the inelastic behavior of concrete. *Mech Mater.*, 4:67-93,1985.
J.L. Chaboche. Development of continuum damage mechanics for elastic solids sustaining anisotropic and unilateral damage. *International Journal of Damage Mechanics*, 2:311-29,1993.
S. Murakami and K. Kamiya. Constitutive and damage evolution-equations of elastic-brittle materials based on irreversible thermodynamics. *Int J Mech Sci.*, 39:473-86:1997.
D. Halm and A. Dragon. An anisotropic model of damage and frictional sliding for brittle materials. *Eur J Mech a-Solid*, 17:439-60,1998.

G. Herrmann and J. Kestin. On the thermodynamics foundation of a damage theory in elastic solids. In: Mazars J, Bazant ZP, editors. *Proceedings of the CNRF-NSK workshop on "Strain localisation and size effect due to damage"*, Amsterdam: Elsevier, 228-32, 1988.
S. Ramtani. Contribution à la modèlisation du comportement multi-axial du bèton endommagè avec description du caractère unilatèral [Ph.D. Thesis]. France: Universite Paris 6, 1990. (in French)
J.H.P. Devree, W.A.M. Brekelmans and M.A.J. Vangils. Comparison of nonlocal approaches in continuum damage mechanics. *Comput Struct.*, 55:581-81,995.
M.G.D. Geers, de Borst R and R.H.J. Peerlings. Damage and crack modeling in single-edge and double-edge notched concrete beams. *Eng Fract Mech.*, 65:247-61,2000.
K.W.E. Warnke. Constitutive model for tri-axial behaviour of concrete. *Proceedings of the concrete structure subjected to tri-axial stresses*, Zurich:1-30,1975.
J.J. Marigo. Modeling of brittle and fatigue damage for elastic-material by growth of microvoids. *Eng Fract Mech.*, 21:861-74,1985.
C. Laborderie and Y. Berthaud. Pijaudier-Cabot G. Crack closure effect in continuum damage mechanics: numerical implementation. *Proceedings of the second international conference on "Computer aided analysis and design of concrete structures"*, Austria:975-86,1990.
J. Lemaitre, R. Desmorat and M. Sauzay. Anisotropic damage law of evolution. *Eur J Mech a-Solid*, 19:187-208,2000.
P. Badel, V. Godard and J.B. Leblond. Application of some anisotropic damage model to the prediction of the failure of some complex industrial concrete structure. *Int J Solids Struct.*, 44:5848-74,2007.
X. Jin and Li Z. Investigation on mechanical properties of young concrete. *Mater Struct.*, 33:627-33,2000.

Appendix A

The secant operator is in fact the effective (damaged) fourth-order elasticity tensor $\overline{C}$ as when no permanent stresses are modeled

$$\boldsymbol{\sigma} = \overline{\mathbf{C}} : \boldsymbol{\varepsilon} \tag{A1}$$

In our case it has the same expression for both local and nonlocal anisotropic damage models. If $\mathrm{tr}\boldsymbol{\varepsilon} > 0$,

$$\overline{\mathbf{C}} = 2G[(\mathbf{I}-\mathbf{D})^{1/2} \otimes (\mathbf{I}-\mathbf{D})^{1/2} - \frac{(\mathbf{I}-\mathbf{D}) \otimes (\mathbf{I}-\mathbf{D})}{3-\mathrm{tr}\mathbf{D}}] + K(1-\mathrm{tr}\mathbf{D})\mathbf{I} \otimes \mathbf{I} \tag{A2}$$

else if $\mathrm{tr}\boldsymbol{\varepsilon} \le 0$,

$$\overline{\mathbf{C}} = 2G[(\mathbf{I}-\mathbf{D})^{1/2} \otimes (\mathbf{I}-\mathbf{D})^{1/2} - \frac{(\mathbf{I}-\mathbf{D}) \otimes (\mathbf{I}-\mathbf{D})}{3-\mathrm{tr}\mathbf{D}}] + K\mathbf{I} \otimes \mathbf{I} \tag{A3}$$

where $G = E/[2(1+\nu)]$ and $G = K/[3(1-2\nu)]$ are the shear and the bulk modulus respectively, and where the special tensor product $\otimes$ is used for two tensors $\mathbf{A}$ and $\mathbf{B}$, $(\mathbf{A} \otimes \mathbf{B})_{ijkl} = A_{ik}B_{jl}$

Appendix B

If the stress is tension, the elements of the tensor $\mathbf{B}$ can be formulated as follows

$$B_{11} = \frac{(1+\nu)}{9}\left(\frac{4}{1-D_1} + \frac{1}{1-D_2} + \frac{1}{1-D_3}\right) + \frac{1-2\nu}{3(1-\eta_1 D_H)}$$

$$B_{12}=B_{21}=-\frac{(1+\nu)}{9}\left(\frac{2}{1-D_1}+\frac{2}{1-D_2}-\frac{1}{1-D_3}\right)+\frac{1-2\nu}{3(1-\eta_1 D_H)}$$

$$B_{13}=B_{31}=-\frac{(1+\nu)}{9}\left(\frac{2}{1-D_1}-\frac{1}{1-D_2}+\frac{2}{1-D_3}\right)+\frac{1-2\nu}{3(1-\eta_1 D_H)}$$

$$B_{22}=\frac{(1+\nu)}{9}\left(\frac{1}{1-D_1}+\frac{4}{1-D_2}+\frac{1}{1-D_3}\right)+\frac{1-2\nu}{3(1-\eta_1 D_H)}$$

$$B_{23}=B_{32}=-\frac{(1+\nu)}{9}\left(-\frac{1}{1-D_1}+\frac{2}{1-D_2}+\frac{2}{1-D_3}\right)+\frac{1-2\nu}{3(1-\eta_1 D_H)}$$

$$B_{33}=\frac{(1+\nu)}{9}\left(\frac{1}{1-D_1}+\frac{1}{1-D_2}+\frac{4}{1-D_3}\right)+\frac{1-2\nu}{3(1-\eta_1 D_H)}$$

If the stress is compression, the elements of the tensor $\mathbf{B}$ can be rewritten as follows

$$B_{11}=\frac{(1+\nu)}{9}\left(\frac{4}{1-D_1}+\frac{1}{1-D_2}+\frac{1}{1-D_3}\right)+\frac{1-2\nu}{3(1-\eta_2 D_H)}$$

$$B_{12}=B_{21}=-\frac{(1+\nu)}{9}\left(\frac{2}{1-D_1}+\frac{2}{1-D_2}-\frac{1}{1-D_3}\right)+\frac{1-2\nu}{3(1-\eta_2 D_H)}$$

$$B_{13}=B_{31}=-\frac{(1+\nu)}{9}\left(\frac{2}{1-D_1}-\frac{1}{1-D_2}+\frac{2}{1-D_3}\right)+\frac{1-2\nu}{3(1-\eta_2 D_H)}$$

$$B_{22}=\frac{(1+\nu)}{9}\left(\frac{1}{1-D_1}+\frac{4}{1-D_2}+\frac{1}{1-D_3}\right)+\frac{1-2\nu}{3(1-\eta_2 D_H)}$$

$$B_{23}=B_{32}=-\frac{(1+\nu)}{9}\left(-\frac{1}{1-D_1}+\frac{2}{1-D_2}+\frac{2}{1-D_3}\right)+\frac{1-2\nu}{3(1-\eta_2 D_H)}$$

$$B_{33}=\frac{(1+\nu)}{9}\left(\frac{1}{1-D_1}+\frac{1}{1-D_2}+\frac{4}{1-D_3}\right)+\frac{1-2\nu}{3(1-\eta_2 D_H)}$$